What leads to direct epoxidation? An exhaustive DFT investigation of electrophilic oxygen mediated epoxidation of ethylene on Ag(100)

Aathira Nair[†,‡] and Kavita Joshi[*,†,‡]

†*Physical and Materials Chemistry Division, CSIR-National Chemical Laboratory, Dr. Homi Bhabha Road, Pune-411008, India.*

‡*Academy of Scientific and Innovative Research (AcSIR), Sector 19, Kamla Nehru Nagar, Ghaziabad, Uttar Pradesh- 201002, India*

E-mail: k.joshi@ncl.res.in

Abstract

Extensive research has contributed to a better understanding of the commercially important epoxidation reaction. Selectivity, a crucial aspect of this reaction, has received significant attention in both experimental and theoretical investigations. However, a consensus regarding the role of electrophilic oxygen in epoxidation is yet to be reached. The present study is a theoretical examination of the prerequisites necessary for direct epoxidation to occur on the Ag(100) surface, at varied monolayer concentrations. Additionally, the study investigates the characteristics of various oxygen species interacting with ethylene to promote the direct epoxidation pathway. Based on the effective charges and projected density of states (pDOS) analysis, three oxygen variants

were identified on the Ag(100) surface: atomic oxygen, dissociatively adsorbed molecular oxygen, and O_3. The investigation reveals that all oxygen species, despite their physical and electronic differences, are electrophilic and undergo direct epoxidation. This work provides insights into the electronic factors influencing the epoxidation on Ag-O complexes.

Keywords

DFT, direct epoxidation, Ethylene Oxide (EtO), OMC, Ag(100), electrophilic oxygen.

Introduction

Epoxidation is one of the most commercially relevant reactions, extensively studied to improve productivity and match market economics. This reaction is known to be affected by factors such as surface coverage, catalyst, subsurface oxygen, and the nature of adsorbed oxygen. Many attempts were made to identify the nature of oxygen that participates in epoxidation on the silver surface, and several studies were carried out to prove it both experimentally and theoretically.[1–39] Some earlier works focus on the physical and electronic properties of oxygen variants on silver, affecting selective epoxidation. In one such investigation, adsorbed O and dissolved O were found as necessary conditions for producing ethylene oxide by unsupported and unpromoted Ag(111) facet.[4] The study predicts partial and total oxidation routes and correlates them with differences in the effective charge on adsorbed oxygen. Oxygen with a higher effective charge was said to initiate total oxidation by cleaving the C-H bond of ethylene. They also propose that selective oxidation results from the electrophilic attack of oxygen on the olefinic bond of ethylene.[4] Analogous to the observations made in this study, another set of experiments presented electrophilic oxygen as atomic species adsorbed on the surface of Ag with lesser charge gains than nucleophilic oxygen.[11] In yet another examination, it was proposed that ethylene reacts with weakly bound oxygen

by adsorbing to the Ag catalyst. Also, the oxygen species firmly bound to low-charged Ag atoms prefer a non-selective product in epoxidation.[5]

The XPS experiments differentiated oxygen species on the Ag surface based on their binding energies and effective charges. Atomic oxygen with O 1s BE 528 eV was considered ionic, accountable for ethylene adsorption on the Ag surface; in contrast, covalent atomic oxygen on the surface with BE 530 eV was regarded as the participant in EtO formation.[7,8] Another study illustrates Ag-O bonding to be only ionic with all Ag-O interactions amounting to lower O 1s binding energies (than 528 eV)[31] thus, contradicting the earlier works.[7,8] In situ experiments performed on Ag(110) predict two oxygen variants to participate in epoxidation: a covalently bonded oxygen with BE in the range 530-531 eV and atomic oxygen on an unreconstructed Ag(110) with BE $<$ 528 eV at low coverages($<$0.04 ML).[34] Thus, the polarities in the observations made from BE for oxygen species participating in epoxidation are evident in these investigations. Further, a study combining experiments and quantum chemical calculations for Ag(111) deduced that nucleophilic oxygen favoring total oxidation forms by adsorption-assisted surface reconstruction and resembles bulk oxide. Moreover, it was deduced that electrophilic oxygen responsible for selective oxidation is most likely to form without reconstruction.[22,23] In contrast, combined experimental and theoretical investigations in later years do not observe oxygen at the unreconstructed surface, known to prefer a partial oxidation route but predict oxygen induced reconstructions on the Ag surface under oxygen atmosphere.[32] Some of the research works also highlight the role of subsurface oxygen in favoring ethylene epoxidation. The subsurface oxygen was deduced to compete with the charge on adsorbed oxygen, thereby favoring selective oxidation.[4] Nevertheless, ethylene was also predicted to repel away from adsorbed oxygen in the absence of subsurface oxygen.[6] The oxygen between the top and second silver layers was assigned with BE 528.2 eV in the XPS studies[11] and was anticipated to have significant covalent properties than being purely ionic as considered in previous experimental investigations.[7,8]

Considering the immense literature available for Ag-O interaction and their effect in se-

lective epoxidation, we observe more emphasis on facets like Ag(111) and Ag(110) owing to their thermodynamic stability. We also note the contradictions in the characterization of oxygen over the years on the Ag surface, such as the nature of Ag-O bonding, binding energy values, nature of oxygen participating in partial oxidation and surface reconstruction.[7,8,22,23,31,33,34] Therefore, the nature of oxygen participating in partial and total oxidation is still being determined and needs to reach a common ground. Apart from these factors, the investigations also show the impact of surface coverage in determining selectivity. One of the Density functional theory (DFT) studies observe oxygen coverage greater than 33 % to suppress ethylene adsorption on the metallic part of Ag surface. The activation barrier for OMC formation reduces at this coverage and the mechanism changes to Eley–Rideal where gas phase ethylene interacts with pre-adsorbed oxygen resulting in better yield.[26] Ethylene oxide (EtO) formation can also occur directly without the intermediate formation (oxametallacycle) at higher monolayer coverages. This direct pathway prevents the activation of C-H bonds, consequently preventing the formation of acetaldehyde.[28]

In addition to the observed trends for Ag(111) and Ag(110) facet, there are also notable studies that have explored the Ag(100) facet.[20,21,36] An experimental investigation by Rocca et al. assigns the oxygen just below the topmost atoms of Ag(001) surface as O530 and O528 to oxygen just above the 4FH site based on XPS binding energies and deduces both the species to show different chemical reactivity.[13] The study states that the oxidation state for both species is comparable and that the shift in BE results from an additional interaction of O530 with Ag. They report that the surface induces missing row reconstructions upon dosing oxygen at 150K.[13] Our work observes similar oxygen species, where one binds to surface Ag atoms and the other moves slightly below the surface. Although oxygen-induced surface reconstruction is present, it is distinguishable from missing row-type reconstruction. Another study investigated the interaction between oxygen and Ag surface at different surface cells (1x1, 2x2; and $2\sqrt{2}$x$\sqrt{2}$) by employing DFT.[20] The study deduced the 4FH site as energetically favorable for oxygen adsorption on Ag(100) and that the subsurface oxy-

gen considerably impacts the surface structure. The experimental findings demonstrate that nanowires primarily consisting of the Ag(100) facet display improved selectivity towards ethylene oxide (EtO).[40] Moreover, kinetic and DFT studies across various facets of Ag indicate that the Ag(100) facet, particularly at higher oxygen coverage, exhibits the highest selectivity. Additionally, it is predicted to possess high reactivity, stable oxygen adsorption, and a low activation barrier for epoxidation.[36,39] These collective outcomes emphasize the need for further comprehensive investigation and study of the Ag(100) facet.

Thus, the focus of our study is to investigate the Ag(100) facet and gain insights of different oxygen species on the reconstructed Ag surface, particularly in their interaction with ethylene for direct epoxidation. It is important to note that the reconstruction of the Ag(100) facet is induced in presence of oxygen and is not manually created. Our previous work on Ag-O interaction considered the electrophilic nature of the relatively positive charged species (central O of O_3 adsorbed on the Ag surface), while giving less emphasis to the properties of other oxygen moieties.[38] Recognizing this limitation and the potential artifact of using a 2X2 supercell to capture surface reconstruction trends, we revisit the interactions between Ag and oxygen. DFT is employed to identify distinct oxygen variants formed at different monolayer concentrations. DFT enables the examination of nuances in the system's structural and electronic properties, which can be challenging to investigate experimentally. Additionally, we explore the interaction between ethylene and these oxygen variants, focusing on direct epoxidation. While our primary objective is to understand the interplay between ethylene and adsorbed oxygen favoring direct epoxidation, we also investigate non-selective interactions and discuss the factors that hinder direct epoxidation. To our knowledge, oxygen of different forms (atomic, dissociatively adsorbed and O_3) at different adsorption sites and their interaction with ethylene in various possible orientations are not extensively studied utilizing DFT on Ag(100). The goal is to gain a comprehensive understanding of the interactions taking place on the Ag(100) surface and shed light on how the orientation of ethylene influences the outcome, regardless of the specific oxygen involved. We

aim to build upon the existing literature by expanding our understanding of the necessary conditions for the epoxidation reaction to occur.

Computational Details

All the calculations are carried out within the Kohn-Sham formalism of Density Functional Theory. Projector Augmented Wave potential[41,42] is used, with Perdew Burke Ernzerhof (PBE)[43] approximation for the exchange-correlation and generalized gradient approximation,[44] as implemented in planewave, pseudopotential based code, Vienna Ab initio Simulation Package (*VASP*).[45–47] Van der Waals corrections are applied to account dynamic correlations between fluctuating charge distribution by selecting Grimme method (DFT-D2).[48] Additionally dipole corrections are also incorporated in the slab. Ag(100) is modeled as slab by cleaving a surface with 4 layers in (100) direction with ASE keeping the bottom layer fixed[49] forming 3x3x4 supercell. We have also tested that the trends remain unchanged even if we model the slab as 4x4x4 or 3x3x5, i.e. either by choosing a larger supercell or increasing the number of layers. 20 Å of vacuum added along z-direction of the crystal is sufficient to avoid interaction between adjacent images of planes along this direction. Geometry optimization is carried out with a force cutoff of 0.01 eV/Å on the unfixed atoms and the total energies are converged below 10^{-4} eV for each SCF cycle. A Monkhorst-Pack grid of 6x6x1 is used for Ag(100) facet as k-mesh which resulted in 36 k-points in IBZ (Irreducible Brillouin Zone). Adsorption energy (E_{ads}) is calculated according to formula: E_{ads} = E_{Ag-O} - (E_{slab} + N*E_O/2). Here, E_{Ag-O} is the energy of the surface with adsorbed oxygen, E_{slab} is the energy of the bare surface and E_O is the energy of the molecular oxygen. N =1, 2 or 3 depending on the number of oxygens present on the modeled surface. To compute the pDOS, Löwdin charges on individual atoms, and Crystal Orbital Overlap Population (COOP), LOBSTER package is employed.[50–53] COOP is a bond detection tool which indicates bonding interactions by a positive sign (gain in overlap) and antibonding contributions

with a negative sign.

Results and Discussion

The study is presented in two sections. In the first section we discuss interaction of oxygen with Ag(100) facet at different ML coverages and identify distinct Ag-O complexes. In the subsequent section, interaction of ethylene with these distinct Ag-O complexes is investigated to understand the prerequisite for direct epoxidation.

Ag-O interaction as a function of monolayer coverage

To understand Ag-O interactions, we have taken Ag(100) slab of size 3x3 with a thickness of 4 layers on which the monolayer concentration (ML) of oxygen is varied from 0.11 to 0.33. Overall, 31 optimizations are conducted of which; 4 were for the 0.11ML system, 8 for 0.22ML, and 19 for the 0.33ML system. Various combinations involving oxygen at 4FH (4-fold hollow), 2FB (2-fold bridge), and 1FT (1-fold top) sites (for atomic as well as the molecular form of oxygen) were adopted for optimization at 0.22ML and 0.33ML coverage. We differentiated the configurations based on oxygen coordination with Ag atoms, effective charge, and form of adsorbed oxygen moieties i.e. atomic or molecular. The configurations representing distinct classes are shown in Fig.1, Fig.2, and Fig.3 while, all the other configurations are shown in SI (SI-Fig.1, SI-Fig.2, and SI-Fig.3).

To simulate 0.11ML coverage, one oxygen atom was placed on Ag surface at different sites like hollow (4FH, both symmetrically and unsymmetrically), bridge (2FB), and top (1FT). Oxygen placed at ontop (1FT) and bridge (2FB) sites relocates itself to higher coordinated sites, such as, 4FH or 3FH (3-fold hollow) upon optimization and induces surface reconstruction. These configurations are energetically favorable over symmetrically adsorbed oxygen atoms at the 4FH site, as shown in Fig.1.

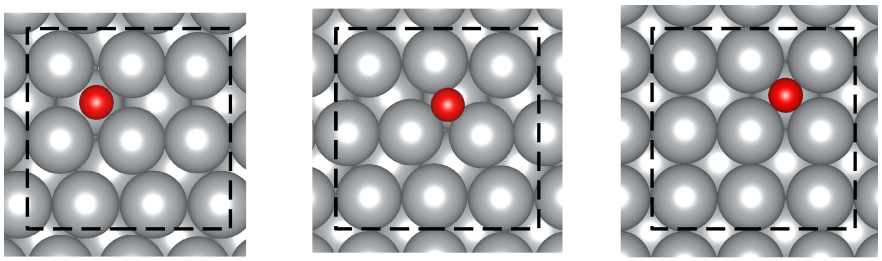

Figure 1: Ag-O interactions at 0.11ML coverage. Oxygen does not stabilize at ontop or bridge site instead; accommodates itself at a 4FH site by inducing reconstruction on the surface. The induced reconstruction is evident in the first two cases. Refer to SI-Fig.1 for the remaining optimized structure. For symmetrically placed oxygen at 4FH the surface reconstructions are minimal.

Table 1: Adsorption energies (E_{ads}), effective charge on adsorbed oxygen, coordination number (CN) of oxygen with silver atoms, and Ag-O bondlengths are tabulated for 0.11ML coverage. The numbers in the () indicate number of bonds with that bondlength.

System	**E_{ads}(eV)**	**charges (e^-)**	**CN**	**bondlengths (Å)**
1	-2.14	-1.20	4	2.24, 2.25(3)
2	-1.90	-1.15	3	2.14(2), 2.16
3	-1.42	-1.19	4	2.24(4)

Interestingly, when O is adsorbed at the 4FH position, all four Ag-O bonds are identical upon optimization. However, the difference in energy between the 1st and 3rd configurations indicates the energy released upon surface reconstruction. From Table 1, it is evident that the charge variation calculated for oxygen at these hollow sites is very minute irrespective of their coordination. Although the variation in charges among configurations is trivial, the individual Ag-O bond strength weakens with increased coordination. In our previous inspection, we discussed the nature of surface reconstruction on Ag(100) and compared them with that of Ag(111) surface.[39] The study demonstrated that the hexagonal formations of Ag atoms exhibited some similarities with Ag(111). This reconstruction was confirmed not to be an artefact of the model, and a similar surface reconstruction is observed for Ag 3X3X5 and 4X4X4 supercell as well. In the present study, this restructuring on the surface induced by oxygen is predominant for all the configurations. Nevertheless, we acknowledge that the surface reconstruction was not captured in the 2x2 model of Ag(100).[38]

Next, representative cases of oxygen-occupied sites at 0.22ML coverage are elucidated in Fig.2 and rest of the configurations are shown in SI-Fig.2. We observe that the increase in monolayer concentration initiates the tendency of oxygen to migrate towards the subsurface. Thus, at 0.22ML and 0.33ML coverages (forthcoming discussion), we observe penta-coordinated oxygen moieties as well. Analogous to the 0.11ML coverage, the configurations comprising atomic oxygen with higher coordination are energetically more stable. The oxygen atom at 5-fold hollow (5FH) sites is slightly below the Ag surface, yet, the charge variation between oxygen at 4FH and 5FH sites is meager as seen in Table 2. A similar trend for oxygen on Ag(001) was observed in the experimental investigation[13] where the oxidation state for oxygen at 4FH and oxygen below surface were found comparable. Besides atomic oxygen, at 0.22ML coverage, we also note molecularly adsorbed oxygen on the surface. The interaction of oxygen molecules with the surface leads to the weakening of O-O bond (from 1.25Å to $\sim$ 1.4Å) and the O-O bond is almost on the verge of dissociation. Thus, they are referred as O_2-dis henceforth.

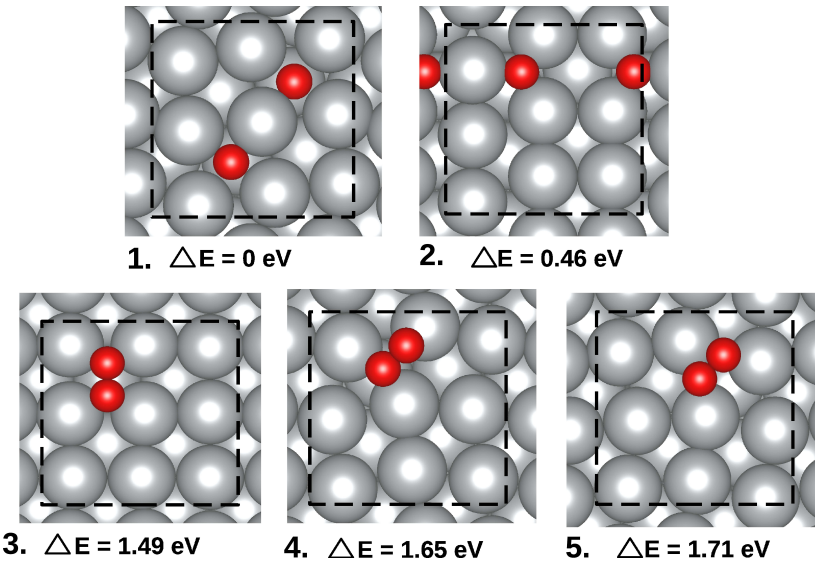

Figure 2: Ag-O interactions at 0.22ML coverage. O_2-dis is also observed for this monolayer coverage. Atomically adsorbed oxygen is energetically more stable than O_2-dis on Ag surface. Refer to SI-Fig.2 for remaining optimized structures.

Table 2: Adsorption energies (E_{ads}), effective charge on adsorbed oxygen, coordination number (CN) of oxygen with silver atoms, and bondlengths for Ag-O and O-O (in case of O_2-dis) are tabulated for 0.22ML coverage. O1 and O2 refers to oxygen atom number 1 and 2 respectively. Properties of O_2-dis are marked in blue color. The numbers in the () indicate number of bonds with that bondlength.

System	**E_{ads}(eV)**	**charges (e^-)**	**CN**	**bondlengths (Å)**
1 (O1)	-3.35	-1.13	4	2.1, 2.21, 2.26, 2.29
- (O2)		-1.15	5	2.11, 2.22, 2.26, 2.3, 2.48
2 (O1)	-2.89	-1.08	3	2.03,2.11(2)
- (O2)		-1.08	3	2.03, 2.11(2)
3 (O1)	-1.86	-0.59	2	2.25(2)
- (O2)		-0.59	2	2.25(2) O-O: 1.43
4 (O1)	-1.69	-0.49	1	2.17
- (O2)		-0.53	2	2.27(2), O-O: 1.39
5 (O1)	-1.64	-0.55	2	2.23, 2.33
- (O2)		-0.55	2	2.23, 2.34, O-O: 1.39

From Table 2, it is observed that for atomic species, the individual Ag-O bond strength reduces as the coordination number (CN) of oxygen increases from 3 to 5. This is reflected in the variation of Ag-O bond length, which ranges from 2.03 Å in 3FH to 2.48 Å in 4/5FH. Similarly, for O_2-dis, the oxygen with CN=2 has weaker Ag-O interaction compared to the oxygen with CN=1, as seen from the variation in Ag-O bondlength from 2.17 Å for CN=1 to 2.34 Å for CN=2. The 4FH site provides greater energetic stability for O_2-dis than the 3FH site. Additionally, a significant charge shift is observed for atomic and dissociatively adsorbed oxygen species (refer to Table 2). As coordination increases, the contribution from each Ag atom reduces towards oxygen, weakening the Ag-O bond strength. Weak Ag-O interaction can facilitate EtO formation and further its removal from surface.

Consonantly, three oxygen atoms (representing 0.33ML coverage) in the combination of both atomic and molecular forms are adsorbed on Ag surface as shown in Fig.3. The increase in monolayer coverage, in this case, also increases the probability of oxygen sliding down the surface layers. As observed at 0.22ML coverage, the energetically most favored structure comprises atomic oxygen at hollow sites. Within configurations exhibiting higher Ag-O coordination, energetically the most stable is the one where two oxygen atoms exhibit four fold coordination. Furthermore, the configuration with all oxygen atoms exhibiting a

5FH coordination is energetically more stable than configurations where two oxygen atoms are positioned at the 3FH site. We also identified O_3 on the Ag surface, which is energetically least probable; however, the electropositive nature of central oxygen makes it noteworthy in this study. The shift in charges for atomic and molecular forms of oxygen is depicted in Table 3. Although reconstruction is observed in all configurations the type of reconstruction is evidently different.

At 0.33ML coverage, all forms of oxygen moieties (atomic, O_2-dis, and O_3) are thermodynamically stable, on Ag(100) facet. However, among these, atomically adsorbed oxygen is energetically the most stable at all monolayer concentrations. The effective charge on the adsorbed oxygen varies depending on the coordination of the oxygen. As observed in instances where oxygen is atomically adsorbed, the coordination ranges from 3 to 5, and the effective charge exceeds $1e^-$. However, when oxygen is adsorbed in its molecular form, the coordination of each individual oxygen atom with silver does not exceed 2.

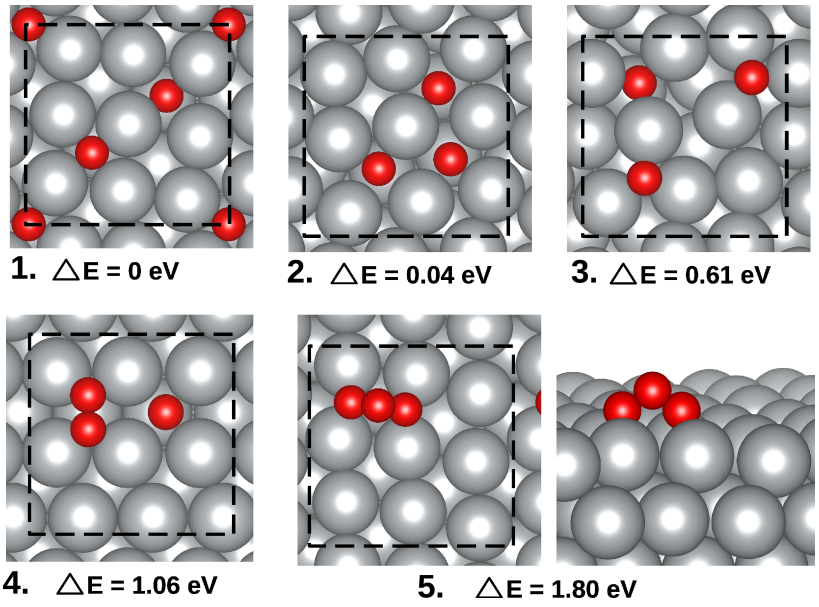

Figure 3: Ag-O interactions at 0.33ML coverage. Adsorbed oxygen can be classified in three forms: atomic, O_2-dis and O_3. O_3 species is energetically the least stable structure. However, the charge on central oxygen of O_3 is relatively positive in comparison to other variants. (Refer to SI-Fig.3) for remaining optimized structures.

Table 3: Adsorption energies (E_{ads}), effective charge on adsorbed oxygen, coordination number (CN) of oxygen with silver atoms, and bondlengths for Ag-O and O-O (in case of O_2-dis and O_3) are tabulated for the 0.33ML system. O1, O2, and O3 refer to oxygen atom numbers 1, 2, and 3, respectively. Properties of O_2-dis are marked in blue, while for O_3, they are marked in red. The numbers in the () indicate the number of bonds with that bondlength.

System	**E_{ads}(eV)**	**charges (e^-)**	**CN**	**bondlengths (Å)**
1 (O1)	-4.6542	-1.14	5	2.09, 2.11, 2.28, 2.31, 2.35
- (O2)		-1.10	4	2.10, 2.18, 2.27, 2.24
- (O3)		-1.10	4	2.07, 2.16, 2.28(2)
2 (O1)	-4.6143	-1.14	5	2.16(2), 2.30, 2.32, 2.4
- (O2)		-1.14	5	2.16, 2.19, 2.4, 2.26(2)
- (O3)		-1.17	5	2.18, 2.29, 2.30, 2.36, 2.40
3 (O1)	-4.0489	-1.05	3	2.05, 2.11, 2.19
- (O2)		-1.11	4	2.08(2), 2.10, 2.34
- (O3)		-1.05	3	2.05, 2.11, 2.19
4 (O1)	-3.5888	-0.54	2	2.21, 2.34
- (O2)		-0.54	2	2.22, 2.34 , O-O: 1.4
- (O3)		-1.17	5	2.20(2), 2.30(2), 2.37
5 (O1)	-2.8534	-0.60	2	2.25, 2.26
- (O2)		-0.60	2	2.26(2)
- (O3)		0.00	2	O-O: 1.4(2)

Consequently, the effective charge acquired by oxygen falls within the range of 0.5 to $0.6e^-$. Lastly, it is worth noting that the central oxygen atom in O_3 remains charge-neutral. Regardless of their form, all these oxygen moieties are charge deficient and electrophilic. Our study suggests that the interaction of oxygen with Ag surface has both covalent and ionic characteristics, with charge transfer occurring from silver to oxygen due to the electronegativity difference between them, and the charge on oxygen being obtained via increased coordination, particularly in the case of oxygen species at hollow sites. This difference in the form of adsorbed oxygen moieties (i.e. atomic/molecular/O_3) also reflects in their respective pDOS. The characteristics of pDOS are common depending upon the effective charge but are independent of ML coverage.

In Fig.4 we plot pDOS of atomic oxygen, O_2-dis, and O_3 at varying monolayer coverages. Fig.4(a), (b), and (c) represents atomically adsorbed oxygen at hollow sites while (d) and (e) depict the pDOS for oxygen of O_2-dis. The pDOS for oxygen of O_3 is shown in Fig.4(f).

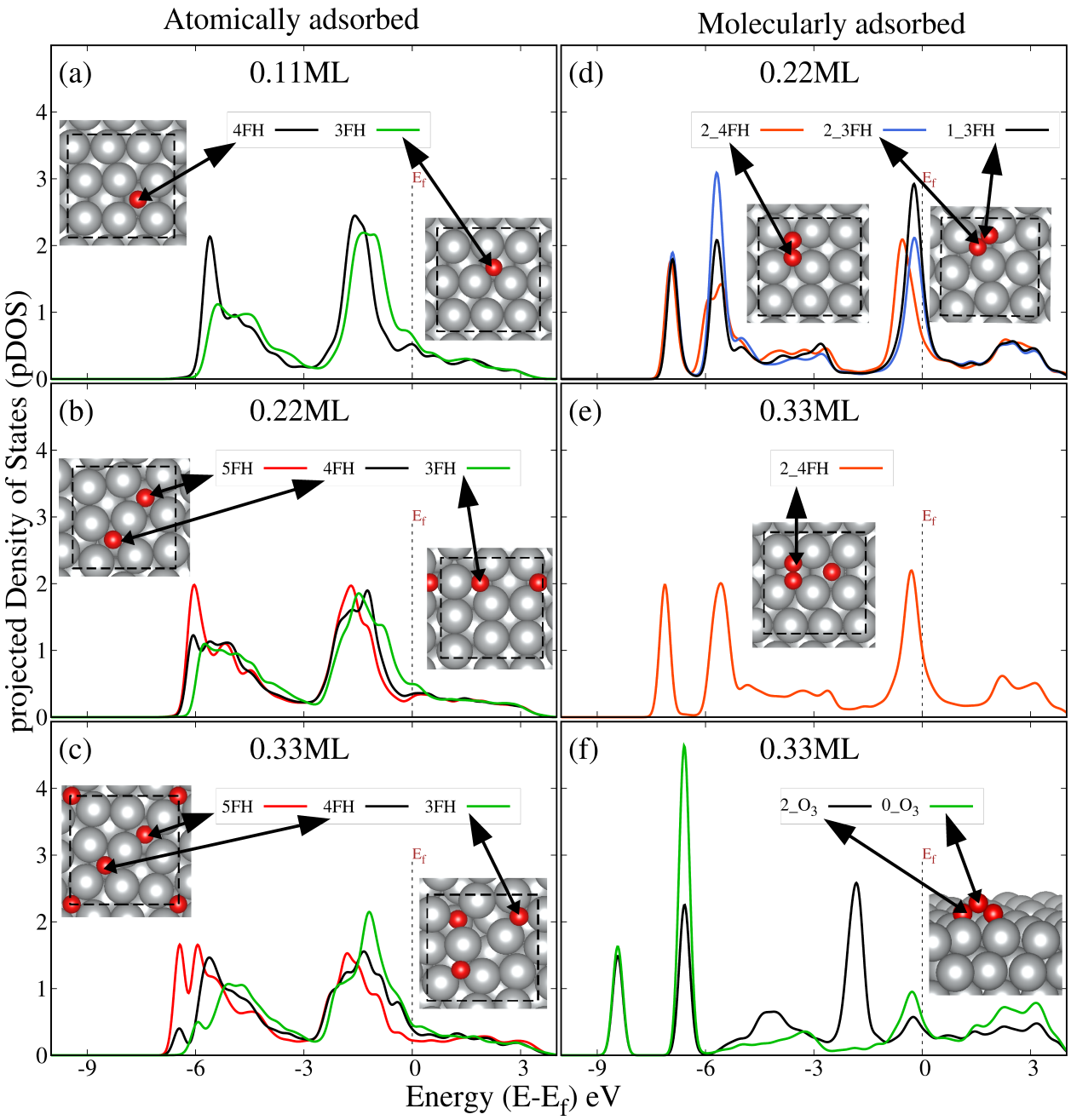

Figure 4: (a), (b), and (c) represents pDOS patterns of oxygen atoms adsorbed at hollow sites in 0.11ML, 0.22ML, and 0.33ML while (d) and (e) depict pDOS for O_2-dis at 0.22ML, and 0.33ML coverages respectively. (f) represents the pDOS for O_3. 3FH (3-fold hollow), 4FH (4-fold hollow), and 5FH (5-fold hollow) represent the site where atomic oxygen adsorbs on the surface. For O_2-dis the numbers 1 and 2 represent the coordination number of the oxygen with Ag. Respective configurations are shown in the inset. The pDOS is distinct for atomic oxygen, O_2-dis, and O_3.

The pDOS for these three oxygen moieties are distinct irrespective of ML concentration.

Two peaks are observed in the pDOS for all atomically adsorbed oxygen moieties, while pDOS for O_2-dis moiety is characterized by three distinct peaks below Fermi. The peaks of O_2-dis and O_3 are sharper than that of atomically adsorbed oxygen. The variation in the intensity of the pDOS peaks upon change in the coordination is more prominent for molecularly adsorbed oxygen than for atomically adsorbed ones. Even though all the oxygen atoms in O_3 show three peaks in their pDOS, the two atoms coordinated with surface have similar peaks to those of O_2-dis, with a slight shift in energy. The central oxygen, however, has a unique pDOS with the sharpest peak in the range of -6 to -7 eV. Interestingly, for all the oxygen variants, the pDOS is non-zero at Fermi, implying that the adsorbed oxygen moieties are interactive and potent towards participating in epoxidation.

Interaction of ethylene with various oxygen moieties

In this section we explore interaction of ethylene with various Ag-O complexes to identify the factors that drive direct epoxidation by electrophilic oxygen. We also discuss cases of non-selective collusions to bring out the difference in initial conditions that leads to distinct outcomes. Although, we have investigated interaction of ethylene with all the distinct configurations, only representative cases are noted here to keep the discussion focused. However, the observations noted are true for the class of configurations that is represented by the case discussed. In the previous section we have shown that adsorbed oxygen moieties can be classified in three groups, atomic, O_2-dis, and O_3. While these three classes are distinct from each other, variation within each class is also observed based on oxygen coordination with Ag (3FH/4FH/5FH) and ML coverage which is evident in pDOS depicted in Fig.4. Effective charge on oxygen is result of all these factors.

We begin by examining how ethylene interacts with atomic oxygen that is adsorbed at hollow sites, leading to direct EtO formation. Ethylene could be placed over atomic oxygen in various different ways. The two distinct ways are based on relative position of carbons of ethylene and adsorbed oxygen. They could be placed equidistant from adsorbed oxygen or

one of the carbons could be placed relatively closer to adsorbed oxygen. We have observed that when both the carbons are placed equidistant from adsorbed oxygen at 0.11ML and 0.22 ML coverage, upon optimization, irrespective of their coordination with surface (i.e. 3/4/5) the product is EtO. In Fig.5 three different initial configurations are shown with adsorbed oxygen placed at 3FH, 4FH, and 5FH. The rest of the configurations resulting into EtO are shown in SI-Fig.4 (O at 4FH) and SI-Fig.5(O at 3FH). We have also explored various relative orientations of ethylene w.r.t. the surface (even if both the carbons are equidistant from adsorbed oxygen) and is demonstrated in all these figures.

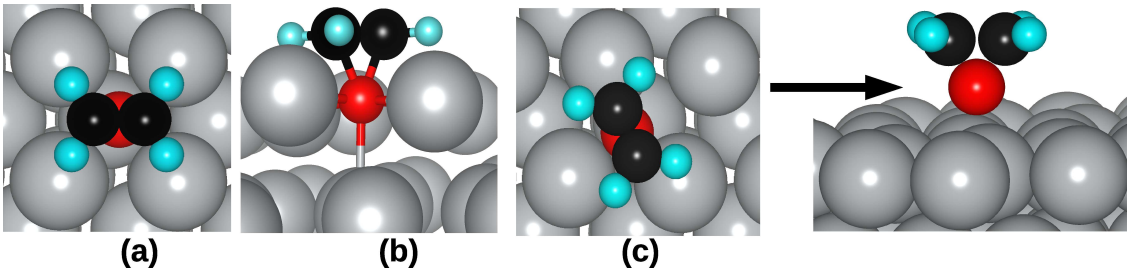

Figure 5: Ethylene is arranged in near symmetric fashion above oxygen at (a) 4FH, (b) 5FH and (c) 3FH site. These orientations initiate EtO formation at all monolayer coverages except for 5FH at 0.33ML coverages.

It can be seen from Fig.5 that in all three cases, carbons of ethylene are approximately equidistant from adsorbed oxygen. Thus, both carbons are available for interaction with oxygen which readily promotes EtO formation. Oxygen at the hollow sites is electrophilic and weakly bonded to the surface. It is also observed that after the formation of EtO, it desorbs from the surface which is crucial and otherwise may lead to OMC formation. We would like to bring to attention an exception to this observation. At 0.33ML coverage the oxygen at 5FH site translates more towards the subsurface region therefore, ethylene fails to interact with the oxygen of this acme regardless of any orientation.

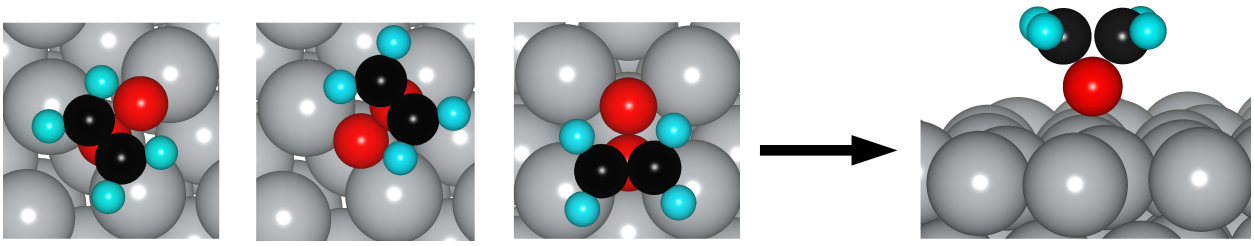

Figure 6: The interplay of ethylene with O_2-dis at 0.22ML and 0.33ML coverage forming EtO is illustrated.

Now we present interaction of O_2-dis with ethylene. Ethylene can be positioned over an O_2-dis in various manners. One way is to align ethylene with one of the oxygen atoms, such that carbon atoms are equidistant from each oxygen but closer to one of them (refer Fig.6). Alternatively, one of the carbons of ethylene can be placed directly above an individual oxygen atom (refer Fig.9). Another possibility is to place ethylene in parallel alignment with the O-O bond, resulting in a one-on-one overlap between a carbon atoms and an oxygen atoms (refer Fig.11). Additionally, ethylene can be arranged in a perpendicular manner, with the C-C bond of ethylene forming a right angle to the O-O bond, or with one of the carbon atoms positioned directly above the O-O bond (refer Fig.13). We have examined all these possibilities and address distinct cases in the forthcoming discussion. Fig.6, depicts representative configurations at 0.22ML and 0.33ML coverage where ethylene is symmetrically placed over one of the atoms of O_2-dis in various possible orientations. As the ethylene molecule approaches the oxygen of O_2-dis, O-O bond dissociates completely. The oxygen which was in proximity of ethylene participates in direct epoxidation while, the other oxygen atom reallocates itself at a new stable hollow site adjacent to its previous location.

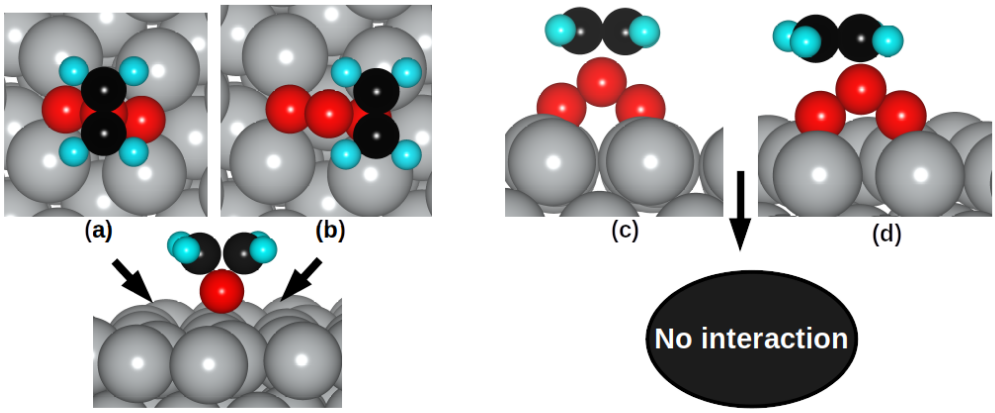

Figure 7: Varied ethylene molecule arrangement above O_3 motif that favor and hinder EtO formation.

We have also investigated interaction of ethylene with the O_3 moiety. Fig.7(a) shows ethylene approaching the central oxygen of O_3, while Fig.7(b) depicts ethylene above an oxygen atom coordinated to the surface, perpendicular to the O_3 motif. Both these cases results into EtO formation. However, in Fig.7(c) and (d), ethylene is placed parallelly above O_3 such that both carbons are at equidistant from the central oxygen in Fig.7(c) and otherwise in Fig.7(d). It is interesting to note that, although ethylene is symmetrically oriented with the central O of O_3 in Fig.7(a) and (c), the environment is different for the two cases resulting into EtO formation in one case and repulsion of ethylene away from the surface in another case. In the case (a), the plane passing through O_3 is perpendicular to the plane passing through ethylene, whereas in (c), the planes of O_3 and ethylene are parallel to one another. A detailed description of electronic effects resulting in the difference in outcomes for case (a) and (c) are discussed in SI-Fig-6. Irrespective of symmetric orientation of ethylene above central oxygen of O_3 the peaks of pDOS represented for both the cases are different from one another. The difference in pDOS peaks for carbons in the lower energy region indicates their difference in environment. Additional peaks are observed for surface oxygen indicating extra interaction in case where ethylene repels. This observation is supported by positive IpCOOP values for carbon and surface oxygen for case (c). The effective charge on central oxygen before ethylene interaction was 0.00 e^- which deviates significantly for case

(a) where the charge is 0.16 e^- compared to case (c) where the charge is -0.02 e^-. Thus interaction of ethylene with central oxygen is more prominent in case (a) than in case (c). In Fig.7(b), ethylene approaches the oxygen adsorbed to the Ag surface almost equidistantly, resembling cases where EtO formation occurs. In Fig.7(d) however, only one carbon is above the central oxygen of O_3, leading to an asymmetric overlap that does not lead to EtO or OMC formation as the carbon is relatively away from the central oxygen and the surface.

Next, we discuss some general trends in the electronic structures associated with the initial configuration of the systems where EtO, OMC and DMC forms.

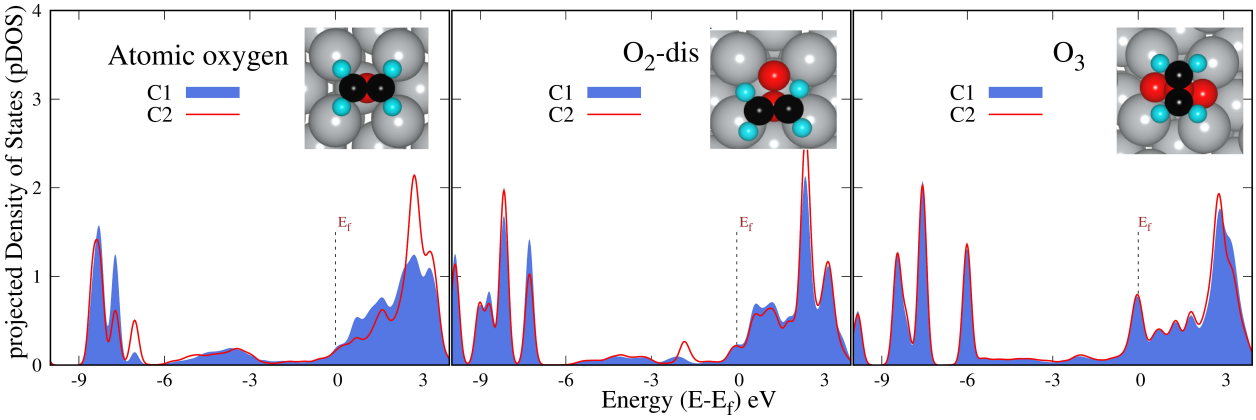

Figure 8: The pDOS plots for carbons are depicted for different representative cases (atomic, O_2-dis, and O_3) where EtO forms. The pDOS of both the carbons are similar.

Fig.8 depicts the pDOS of the carbons of ethylene in cases where EtO forms upon near-symmetric orientation above adsorbed oxygen. When the carbons approach the adsorbed oxygen in a near-symmetric manner, both carbons of ethylene exhibit similar pDOS (as depicted in Fig.8). The corresponding configurations have been provided in the inset of Fig.8 for clarity. Thus the environment of carbons of ethylene in these cases are similar to each other although peak patterns may vary slightly depending on its interaction with different class of oxygen species. Additionally, we have varied the distance between the adsorbate and the surface in order to confirm that our findings are not simply an artefact of the initial distance.

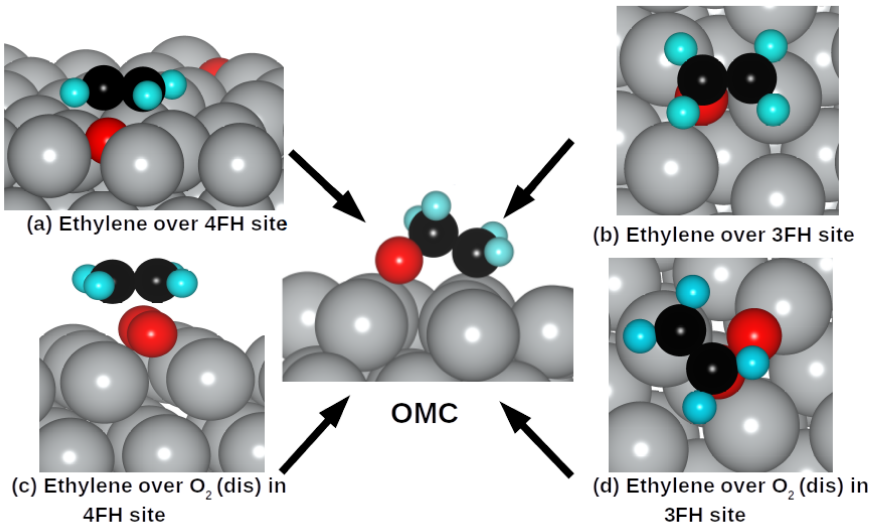

Figure 9: Ethylene interaction with different oxygen variants of the surface that results in oxametallacycle intermediate.

Fig.9 depicts the asymmetric approach of ethylene molecules on different oxygen species. In these cases ethylene molecule is positioned so that one of the carbons of ethylene is closer to the adsorbed oxygen. All the orientations depicted triggers oxametallacycle intermediate formation.

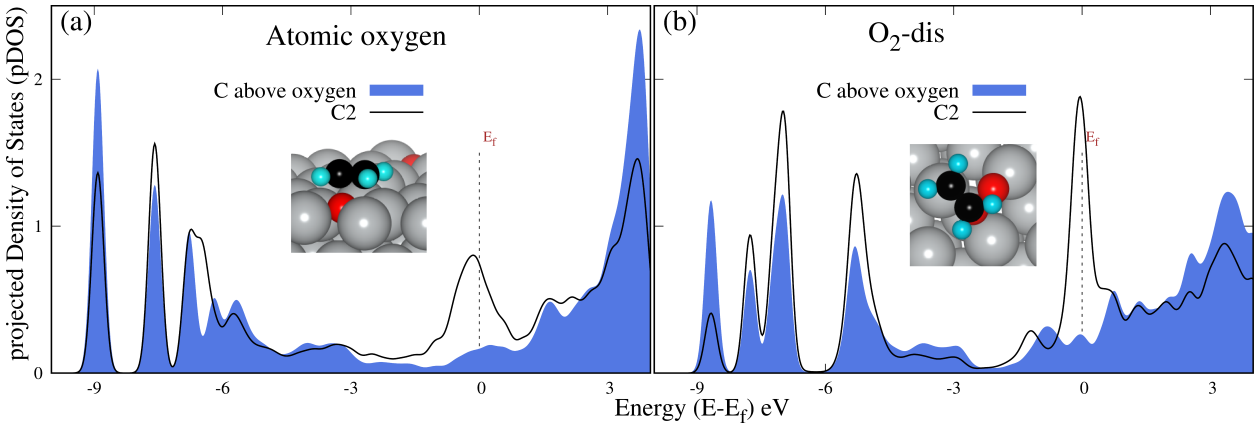

Figure 10: The pDOS plots for carbons of ethylene when placed asymmetrically above adsorbed oxygen are depicted for atomic and O_2-dis case. The corresponding configurations are given in the inset. The peak patterns are dissimilar for the carbons as they are in a different environments.

A clear distinction exists between the pDOS of the carbons atoms in these situations, which differentiates them from scenarios where EtO is formed. Fig.10(a) and (b) demonstrate

the pDOS for the asymmetric approach of ethylene over atomically adsorbed oxygen at the 4FH site and O_2-dis at the 3FH site, respectively. Although the peaks for the carbons of ethylene in these cases do overlap with one another, they are distinct. Additionally, a peak near the Fermi level is observed for the carbon relatively away from the adsorbed oxygen, which is absent for the carbon of ethylene above the oxygen. This observation confirms that the carbons have different environments.

In the preceding discussion, we have covered some general observations regarding the interaction between ethylene and oxygen. Additionally, details on some exceptional cases (not discussed in the main text) where asymmetric interaction of ethylene above adsorbed oxygen forms EtO as product are illustrated in SI-fig.7 and 8. These cases emphasise the role of orientation and reconstruction in differentiating the outcomes irrespective of the adsorbed oxygen involved in the reaction being same. Thus, we note that beyond orientation of ethylene there are also other factors that influence the formation of EtO. Till now most of the focus has been on the formation of EtO and OMC intermediates, regardless, we have also observed the formation of a di-oxametallacycle (DMC) intermediate, which is depicted in Fig.11(a) and (b).

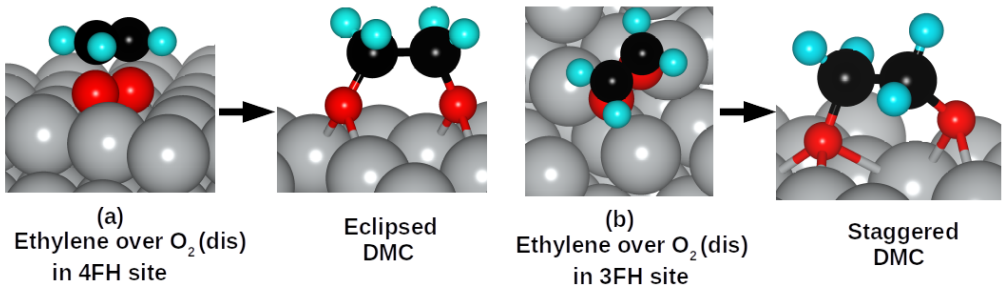

Figure 11: Approach of ethylene molecule parallel to O_2-dis results in dioxometallacycle intermediate (DMC). (a) Moreover, (b) depicts the orientation that forms eclipsed DMC and staggered DMC, respectively.

Figures 11(a) and (b) illustrate the parallel arrangement of ethylene molecules over O_2-dis on the 4FH and 3FH sites of the Ag surface, respectively such that there is one-on-one carbon-oxygen interaction. The resulting association of ethylene and oxygens leads to the

formation of an eclipsed DMC intermediate when O_2-dis is symmetrically adsorbed at the 4FH site, while a staggered DMC intermediate is formed when O_2-dis is adsorbed at the 3FH site. The structural information for DMC is given in SI-Tab.1.

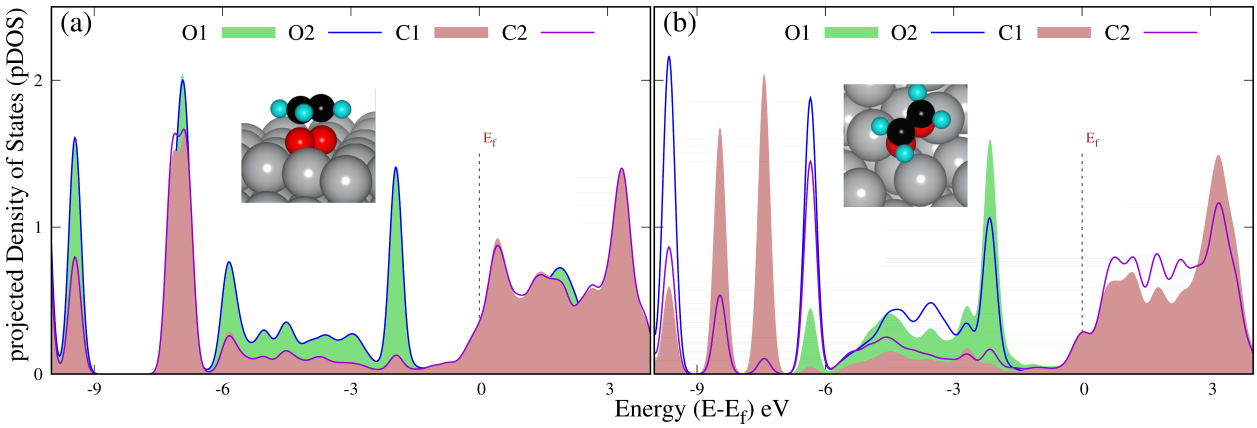

Figure 12: The pDOS patterns for ethylene placed parallelly above O_2-dis are shown. The peak patterns confirm one-on-one interaction between carbon and oxygen for the initial configuration.

The pDOS plots depicted in Fig.12 provide insights into the interaction between carbon and oxygen by displaying the overlap of peak patterns. The peaks for oxygen (O1 and O2) and carbon (C1 and C2) display similar patterns, indicating a one-on-one overlap and similar individual peaks for both elements. Therefore, in cases where DMC is formed, two sets of peaks representing two O-C interactions can be observed. However, for the 3FH site, the variations in the pDOS are linked to an asymmetric 3FH adsorption site for oxygen, where the coordination number of both the oxygen atoms with Ag is different. On the other hand, in the case of O_2-dis at a symmetric 4FH site, there is a complete overlap of oxygen and carbon pDOS. Here, although the carbons of ethylene show similar environment in pDOS the result is not EtO.

Furthermore, we have discussed the cases in which ethylene fails to interact with the oxygen of O_2-dis. In these cases, the ethylene molecule is arranged in such a way that it is parallel to the surface and perpendicular to the O-O bond of the O_2-dis motifs, as shown in Fig.13(a), (b) and (c). All three arrangements fail to result in any relevant product as they

shift away from the oxygen groups.

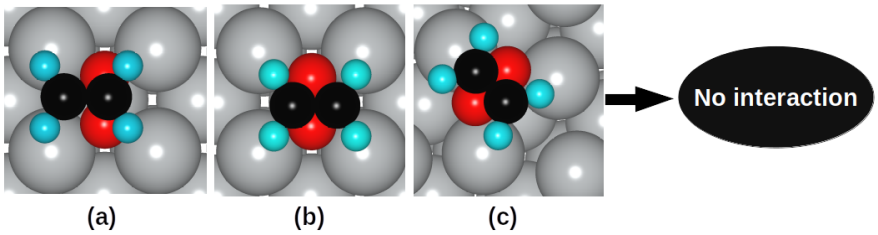

Figure 13: Arrangement of ethylene molecules above dissociated oxygen species that fail to interact with each other. (a) and (b) represents ethylene above O_2-dis at 4FH site and (c) represents O_2-dis at 3FH site.

We considered O_2-dis systems in which oxygens are symmetrically adsorbed at both the 4FH and 3FH sites, with the latter being less stable due to unsymmetrical adsorption. Nevertheless, we utilized it as a reference to comprehend the effect. The arrangement of the ethylene molecule above the dissociated O_2 motifs was such that they were parallel to the surface and perpendicular to the O-O bond, as shown in Fig.13(a), (b), and (c). In Fig.13(a), one of the carbons of ethylene was positioned above the O-O bond, whereas in Fig.13(b) and (c), both carbons of the ethylene molecule were equidistant from the O_2-dis moiety, resulting in a similar environment to that of Fig.13(a). However, all three arrangements failed to facilitate ethylene-oxygen interaction as they shifted away from the oxygen groups, resulting in no relevant product.

In this study, we find that subsurface oxygen is not necessary for EtO formation on Ag(100) facet. Even at low surface coverages (0.11ML), EtO is formed on the surface without subsurface oxygen, contradicting earlier studies on different facets that showed ethylene interaction to be repulsive without subsurface oxygen.[6] Our results show that all oxygen species, irrespective of charge variations and coordination, form EtO. We also observe that oxygen adsorbs on the reconstructed Ag(100) surface in all cases yet successfully forms EtO upon favorable ethylene interaction. This observation differs from the earlier works on different facets.[22,23] Our analysis suggests a combination of covalent and ionic bonding associated with Ag-O interaction. The importance of ethylene orientation in driving direct epoxidation,

alongside other factors that impact the selectivity of ethylene oxide, is emphasized in this study.

Conclusion

In this study, we employed density functional theory to explore the interactions between O and the Ag(100) surface, classifying them based on their distinct characteristics. Our findings demonstrate the existence of three types of oxygen moieties on the Ag surface: atomic, O_2-dis, and O_3. Irrespective of ML coverage, atomic oxygen is thermodynamically most favored however, we have explored ethylene interaction with all the three Ag-O complexes. Despite differences in charges, all identified oxygen moieties exhibit electrophilic properties. We predict a combination of ionic and covalent interactions between adsorbed oxygen and coordinated silver. Our observations indicate that the presence of oxygen triggers surface reconstruction on the Ag(100) surface, with a greater distortion occurring as the monolayer coverage increases. The focus of our study is to enhance our understanding of the interactions between Ag and oxygen and to clarify the prerequisites that enable oxygen to participate in the epoxidation process.

It is worth noting that all electrophilic variants form on the reconstructed Ag surface. Their interaction with ethylene leads to EtO irrespective of the effective charge on oxygen and ML concentration. Direct epoxidation depends upon the relative orientation of ethylene with respect to surface oxygen. Asymmetric interaction of ethylene with adsorbed oxygen leads to the formation of products such as oxametallacycle and dioxo-metallacycle (DMC), and sometimes fails to interact. However, we discuss exceptional cases where partial overlap results in EtO formation, including the interaction of ethylene on energetically less probable O_3. The computed pDOS and COOP are in line with our observations. In conclusion, our study reveals that direct epoxidation can proceed on all types of electrophilic oxygen variants, with ethylene adopting a near symmetric approach above the adsorbed oxygen. However, not

all interactions of ethylene favor epoxide formation, and result in the formation of products that hinder direct epoxidation. Our study provides new insights into the conventions that affect the selectivity of EtO.

Acknowledgments

Authors thanks CSIR project MLP100526 (Understanding reaction mechanism in ethylene epoxidation) for financial support. CSIR-4PI is greatfully acknowledged for providing computational resources.

References

(1) Twigg, G. H. The catalytic oxidation of ethylene. *Trans. Faraday Soc.* **1946**, *42*, 284–290.

(2) Force, E. L.; Bell, A. T. The relationship of adsorbed species observed by infrared spectroscopy to the mechanism of ethylene oxidation over silver. *Journal of Catalysis* **1975**, *40*, 356 – 371.

(3) Backx, C.; Moolhuysen, J.; Geenen, P.; Van Santen, R. Reactivity of oxygen adsorbed on silver powder in the epoxidation of ethylene. *Journal of Catalysis* **1981**, *72*, 364–368.

(4) Grant, R. B.; Lambert, R. M. A single crystal study of the silver-catalysed selective oxidation and total oxidation of ethylene. *Journal of Catalysis* **1985**, *92*, 364–375.

(5) Van Santen, R.; Kuipers, H. The mechanism of ethylene epoxidation. *Advances in Catalysis* **1987**, *35*, 265–321.

(6) Van den Hoek, P.; Baerends, E.; Van Santen, R. Ethylene epoxidation on silver (110): the role of subsurface oxygen. *The Journal of Physical Chemistry* **1989**, *93*, 6469–6475.

(7) Bukhtiyarov, V.; Boronin, A.; Savchenko, V. Two oxygen states and the role of carbon in partial oxidation of ethylene over silver. *Surface Science* **1990**, *232*, 205–209.

(8) Bukhtiyarov, V.; Prosvirin, I.; Kvon, R. Study of reactivity of oxygen states adsorbed at a silver surface towards C_2H_4 by XPS, TPD and TPR. *Surface Science* **1994**, *320*, 47–50.

(9) Bao, X.; Muhler, M.; Schedel-Niedrig, T.; Schlögl, R. Interaction of oxygen with silver at high temperature and atmospheric pressure: A spectroscopic and structural analysis of a strongly bound surface species. *Phys. Rev. B* **1996**, *54*, 2249–2262.

(10) Avdeev, V. I.; Boronin, A. I.; Koscheev, S. V.; Zhidomirov, G. M. Quasimolecular stable forms of oxygen on silver surface. Theoretical analysis by the density functional theory method. *Journal of Molecular Catalysis A: Chemical* **2000**, *154*, 257 – 270.

(11) Bukhtiyarov, V.; Kaichev, V.; Prosvirin, I. Oxygen adsorption on Ag (111): X-ray photoelectron spectroscopy (XPS), angular dependent x-ray photoelectron spectroscopy (ADXPS) and temperature-programmed desorption (TPD) studies. *The Journal of Chemical Physics* **1999**, *111*, 2169–2175.

(12) Bukhtiyarov, V.; Kaichev, V. The combined application of XPS and TPD to study of oxygen adsorption on graphite-supported silver clusters. *Journal of Molecular Catalysis A: Chemical* **2000**, *158*, 167 – 172.

(13) Rocca, M.; Savio, L.; Vattuone, L.; Burghaus, U.; Palomba, V.; Novelli, N.; de Mongeot, F. B.; Valbusa, U.; Gunnella, R.; Comelli, G., et al. Phase transition of dissociatively adsorbed oxygen on Ag (001). *Physical Review B* **2000**, *61*, 213–228.

(14) Bukhtiyarov, V. I.; Hävecker, M.; Kaichev, V. V.; Knop-Gericke, A.; Mayer, R. W.; Schlögl, R. X-ray absorption and photoemission studies of the active oxygen for ethylene epoxidation over silver. *Catalysis Letters* **2001**, *74*, 121–125.

(15) Suljo, L.; A., B. M. Formation of a Stable Surface Oxametallacycle that Produces Ethylene Oxide. *Journal of the American Chemical Society* **2002**, *124*, 310–317.

(16) Linic, S.; Barteau, M. A. Construction of a reaction coordinate and a microkinetic model for ethylene epoxidation on silver from DFT calculations and surface science experiments. *Journal of Catalysis* **2003**, *214*, 200 – 212.

(17) Linic, S.; Barteau, M. A. Control of Ethylene Epoxidation Selectivity by Surface Oxametallacycles. *Journal of the American Chemical Society* **2003**, *125*, 4034–4035, PMID: 12670209.

(18) Linic, S.; Piao, H.; Adib, K.; Barteau, M. A. Ethylene Epoxidation on Ag: Identification of the Crucial Surface Intermediate by Experimental and Theoretical Investigation of its Electronic Structure. *Angewandte Chemie International Edition* **2004**, *43*, 2918–2921.

(19) Li, W.-X.; Stampfl, C.; Scheffler, M. Oxygen adsorption on Ag(111): A density-functional theory investigation. *Phys. Rev. B* **2002**, *65*, 075407–1–075407–19.

(20) Wang, Y.; Jia, L.; Wang, W.; Fan, K. O/Ag(100) Surface: A Density Functional Study with Slab Model. *The Journal of Physical Chemistry B* **2002**, *106*, 3662–3667.

(21) Wang, Y.; Jia, L.; Dai, W.; Wang, W.; Fan, K. Theoretical study about adsorption of atomic oxygen on unmodified and I-modified Ag (100) surface. *The Journal of Chemical Physics* **2003**, *118*, 11210–11216.

(22) Kaichev, V.; Bukhtiyarov, V.; Hävecker, M.; Knop-Gercke, A.; Mayer, R.; Schlögl, R. The nature of electrophilic and nucleophilic oxygen adsorbed on silver. *Kinetics and Catalysis* **2003**, *44*, 432–440.

(23) Bukhtiyarov, V. I.; Hävecker, M.; Kaichev, V. V.; Knop-Gericke, A.; Mayer, R. W.; Schlögl, R. Atomic oxygen species on silver: Photoelectron spectroscopy and x-ray absorption studies. *Physical Review B* **2003**, *67*, 235422–1–235422–12.

(24) Schnadt, J.; Knudsen, J.; Hu, X. L.; Michaelides, A.; Vang, R. T.; Reuter, K.; Li, Z.; Lægsgaard, E.; Scheffler, M.; Besenbacher, F. Experimental and theoretical study of oxygen adsorption structures on Ag(111). *Physical Review B* **2009**, *80*, 075424–1–075424–10.

(25) Fellah, M. F.; van Santen, R. A.; Onal, I. Epoxidation of Ethylene by Silver Oxide (Ag_2O) Cluster: A Density Functional Theory Study. *Catalysis Letters* **2011**, *141*, 762–771.

(26) Ozbek, M.; Onal, I.; Van Santen, R. Effect of surface and oxygen coverage on ethylene epoxidation. *Topics in Catalysis* **2012**, *55*, 710–717.

(27) Rocha, T. C. R.; Oestereich, A.; Demidov, D. V.; Hävecker, M.; Zafeiratos, S.; Weinberg, G.; Bukhtiyarov, V. I.; Knop-Gericke, A.; Schlögl, R. The silver–oxygen system in catalysis: new insights by near ambient pressure X-ray photoelectron spectroscopy. *Physical Chemistry Chemical Physics* **2012**, *14*, 4554–4564.

(28) Özbek, M.; Van Santen, R. The mechanism of ethylene epoxidation catalysis. *Catalysis Letters* **2013**, *143*, 131–141.

(29) Böcklein, S.; Günther, S.; Wintterlin, J. High-Pressure Scanning Tunneling Microscopy of a Silver Surface during Catalytic Formation of Ethylene Oxide. *Angewandte Chemie International Edition* **2013**, *52*, 5518–5521.

(30) Martin, N. M.; Klacar, S.; Grönbeck, H.; Knudsen, J.; Schnadt, J.; Blomberg, S.; Gustafson, J.; Lundgren, E. High-Coverage Oxygen-Induced Surface Structures on Ag(111). *The Journal of Physical Chemistry C* **2014**, *118*, 15324–15331.

(31) Jones, T. E.; Rocha, T. C. R.; Knop-Gericke, A.; Stampfl, C.; Schlögl, R.; Piccinin, S. Insights into the Electronic Structure of the Oxygen Species Active in Alkene Epoxidation on Silver. *ACS Catalysis* **2015**, *5*, 5846–5850.

(32) Jones, T. E.; Rocha, T. C. R.; Knop-Gericke, A.; Stampfl, C.; Schlögl, R.; Piccinin, S. Thermodynamic and spectroscopic properties of oxygen on silver under an oxygen atmosphere. *Phys. Chem. Chem. Phys.* **2015**, *17*, 9288–9312.

(33) Jones, T. E.; Wyrwich, R.; Böcklein, S.; Rocha, T. C.; Carbonio, E. A.; Knop-Gericke, A.; Schlögl, R.; Günther, S.; Wintterlin, J.; Piccinin, S. Oxidation of ethylene on oxygen reconstructed silver surfaces. *The Journal of Physical Chemistry C* **2016**, *120*, 28630–28638.

(34) Carbonio, E. A.; Rocha, T. C.; Klyushin, A. Y.; Píš, I.; Magnano, E.; Nappini, S.; Piccinin, S.; Knop-Gericke, A.; Schlögl, R.; Jones, T. E. Are multiple oxygen species selective in ethylene epoxidation on silver? *Chemical Science* **2018**, *9*, 990–998.

(35) Jones, T. E.; Wyrwich, R.; Böcklein, S.; Carbonio, E. A.; Greiner, M. T.; Klyushin, A. Y.; Moritz, W.; Locatelli, A.; Menteş, T. O.; Niño, M. A., et al. The selective species in ethylene epoxidation on silver. *ACS Catalysis* **2018**, *8*, 3844–3852.

(36) Huš, M.; Hellman, A. Ethylene epoxidation on Ag (100), Ag (110), and Ag (111): a joint ab initio and kinetic monte carlo study and comparison with experiments. *ACS Catalysis* **2018**, *9*, 1183–1196.

(37) Ghosalya, M. K.; Reddy, K. P.; Jain, R.; Roy, K.; Gopinath, C. S. Subtle interaction between Ag and O_2: a near ambient pressure UV photoelectron spectroscopy (NAP-UPS) investigations. *Journal of Chemical Sciences* **2018**, *130*, 1–11.

(38) Kenge, N.; Pitale, S.; Joshi, K. The nature of electrophilic oxygen: Insights from periodic density functional theory investigations. *Surface Science* **2019**, *679*, 188–195.

(39) Nair, A.; Kenge, N.; Joshi, K. Role of facet in the competitive pathway of ethylene epoxidation. *Surface Science* **2022**, *716*, 121954–1–121954–8.

(40) Christopher, P.; Linic, S. Shape-and size-specific chemistry of Ag nanostructures in catalytic ethylene epoxidation. *ChemCatChem* **2010**, *2*, 78–83.

(41) Blöchl, P. E. Projector augmented-wave method. *Physical Review B* **1994**, *50*, 17953–17979.

(42) Kresse, G.; Joubert, D. From ultrasoft pseudopotentials to the projector augmented-wave method. *Physical Review B* **1999**, *59*, 1758–1775.

(43) Perdew, J. P.; Burke, K.; Ernzerhof, M. Generalized gradient approximation made simple. *Physical Review Letters* **1996**, *77*, 3865–3868.

(44) Perdew, J. P.; Burke, K.; Ernzerhof, M. Generalized gradient approximation made simple [Physical Review Letters 77, 3865 (1996)]. *Physical Review Letters* **1997**, *78*, 1396.

(45) Kresse, G.; Hafner, J. Ab initio molecular-dynamics simulation of the liquid-metal–amorphous-semiconductor transition in germanium. *Physical Review B* **1994**, *49*, 14251–14271.

(46) Kresse, G.; Furthmüller, J. Efficient iterative schemes for *ab initio* total-energy calculations using a plane-wave basis set. *Physical Review B* **1996**, *54*, 11169–11186.

(47) Kresse, G.; Furthmüller, J. Efficiency of ab-initio total energy calculations for metals and semiconductors using a plane-wave basis set. *Computational Materials Science* **1996**, *6*, 15–50.

(48) Grimme, S. Semiempirical GGA-type density functional constructed with a long-range dispersion correction. *Journal of Compuatational Chemistry* **2006**, *27*, 1787–99.

(49) Larsen, A. H. et al. The atomic simulation environment—a Python library for working with atoms. *Journal of Physics: Condensed Matter* **2017**, *29*, 273002–1–273002–30.

(50) Dronskowski, R.; Blöchl, P. E. Crystal orbital Hamilton populations (COHP): energy-resolved visualization of chemical bonding in solids based on density-functional calculations. *The Journal of Physical Chemistry* **1993**, *97*, 8617–8624.

(51) Deringer, V. L.; Tchougréeff, A. L.; Dronskowski, R. Crystal orbital Hamilton population (COHP) analysis as projected from plane-wave basis sets. *The Journal of Physical Chemistry A* **2011**, *115*, 5461–5466.

(52) Maintz, S.; Deringer, V. L.; Tchougréeff, A. L.; Dronskowski, R. Analytic projection from plane-wave and PAW wavefunctions and application to chemical-bonding analysis in solids. *Journal of Computational Chemistry* **2013**, *34*, 2557–2567.

(53) Maintz, S.; Deringer, V. L.; Tchougréeff, A. L.; Dronskowski, R. LOBSTER: A tool to extract chemical bonding from plane-wave based DFT. *Journal of Computational Chemistry* **2016**, *37*, 1030–1035.